THE JOURNAL OF PHYSICAL CHEMISTRY Letters

Letter

pubs.acs.org/JPCL

Alkyl Chain Length and Temperature Effects on Structural Properties of Pyrrolidinium-Based Ionic Liquids: A Combined Atomistic Simulation and Small-Angle X-ray Scattering Study

Song Li,[†] José Leobardo Bañuelos,[‡] Jianchang Guo,[‡] Lawrence Anovitz,[‡] Gernot Rother,[‡] Robert W. Shaw,[‡] Patrick C. Hillesheim,[‡] Sheng Dai,[‡] Gary A. Baker,[§] and Peter T. Cummings*[,†,⊥]

[†]Department of Chemical and Biomolecular Engineering, Vanderbilt University, Nashville, Tennessee 37235, United States

[‡]Chemical Sciences Division, Oak Ridge National Laboratory, Oak Ridge, Tennessee 37831, United States

[§]Department of Chemistry, University of Missouri, Columbia, Missouri 65211-7600, United States

[⊥]Center for Nanophase Materials Science, Oak Ridge National Laboratory, Oak Ridge, Tennessee 37831, United States

Supporting Information

ABSTRACT: Molecular dynamics (MD) simulations of 1-alkyl-1-methylpyrrolidinium bis(trifluoromethanesulfonyl)imide ([C_nMPy][Tf_2N], n = 3, 4, 6, 8, 10) were conducted using an all-atom model. Radial distribution functions (RDF) were computed and structure functions were generated to compare with new X-ray scattering experimental results, reported herein. The scattering peaks in the structure functions generally shift to lower Q values with increased temperature for all the liquids in this series. However, the first sharp diffraction peak (FSDP) in the longer alkyl chain liquids displays a marked shift to higher Q values with increasing temperature. Alkyl chain-dependent ordering of the polar groups and increased tail aggregation with increasing alkyl chain length were observed in the partial pair correlation functions and the structure functions. The reasons for the observed alkyl chain-dependent phenomena and temperature effects were explored.

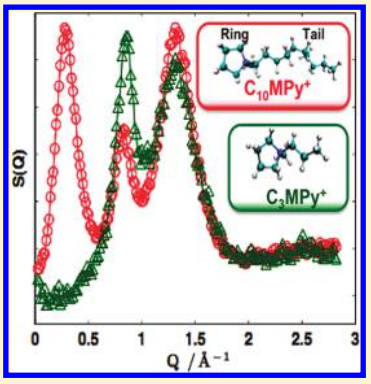

SECTION: Molecular Structure, Quantum Chemistry,General Theory

Room temperature ionic liquids (RTILs), as promising electrolytes and green solvents, have been widely studied in recent years due to their interesting and unique properties such as negligible volatility and high electrochemical and thermal stability.[1,2] Ionic liquids can be tailored to specific applications by fine-tuning the functional groups of the weakly coordinating organic cation and the inorganic/organic anion.[3] It is known that the alkyl chain length of the cation influences both the physical and chemical properties of RTILs. A longer cation side chain is commonly accompanied by lower density, lower solubility, slower diffusion, and higher viscosity.[4−6] Imidazolium-based ionic liquids, one of the most studied RTILs to date, have been reported to exhibit aggregation behavior as a function of alkyl chain length by atomistic/coarse-grained molecular dynamics simulation.[7−10] Small-angle X-ray scattering (SAXS) has been used to identify the presence of liquid crystalline phases in imidazolium-based ionic liquids with $n \geq 12$, depending on the type of anion,[11] while structural heterogeneity has been found in shorter alkyl chain ionic liquids.[12−14] The effect of cation asymmetry on structural heterogeneity[4,15] and several physicochemical properties[16] has also been recently addressed. Small-angle neutron scattering has been used to show that the increased heterogeneity stems primarily from the increasing asymmetry of the cation as the chain length is increased.[17,18]

Recently, 1-alkyl-1-methylpyrrolidinium bis(trifluoromethanesulfonyl)imide ([C_nMPy][Tf_2N], n = 3, 4, 6, 8, 10) has been recognized as an interesting class of ionic liquids due to its wider electrochemical window: up to 5.9 V, compared to the more studied [$C_n$mim][Tf_2N] (4.9 V). Also, [C_nMPy][Tf_2N] exhibits higher electrochemical stability than [$C_n$mim][Tf_2N].[19] Presently, only limited studies, especially computational studies, on pyrrolidinium-based ionic liquids have been reported. The X-ray scattering study by Santos et al.[20] revealed that long alkyl chain [C_nMPy][Tf_2N] homologues display a FSDP for n = 6, 8, and 10, similar to what is observed in [$C_n$mim][Tf_2N].[12] In that study, the FSDP was attributed to intermediate range ordering arising between the first- and second-shell neighbors of the asymmetric ions. Additionally, the shift of structural peaks toward larger distances with increased temperature has been discussed by Santos et al.,[20] but the temperature dependence of the low-Q peak for [C_nMPy][Tf_2N], which exhibits the opposite trend demonstrated in the new experimental data in this paper, has not been previously reported. In earlier work, we observed the dynamic heterogeneity of [C_nMPy][Tf_2N] has been observed using a

Received: September 28, 2011
Accepted: November 22, 2011
Published: November 22, 2011

fluorescence correlation spectroscopy (FCS) method that was more pronounced for homologues with longer alkyl chain length.[21] However, a corresponding computational study of $[C_nMPy][Tf_2N]$ has not been reported, and it would be of interest to see whether the reported heterogeneity probed by FCS can be also observed using MD simulation and other experimental methods. In this paper, we report a combined MD simulation and SAXS study on the liquid structure of pyrrolidinium-based ionic liquids, $[C_nMPy][Tf_2N]$. Self-aggregation of nonpolar alkyl chains appears clearly in long chain $[C_nMPy][Tf_2N]$ ionic liquids, and the resulting alkyl chain-dependent polar group ordering provides a clearer view of the heterogeneous nature of ionic liquid structures.

The all-atom force field developed by Smith's group[22] has been applied here to the $[C_nMPy][Tf_2N]$ ionic liquids. Simulation details are given in the Supporting Information. A cubic simulation box consisting of 125 ion pairs equilibrated at 298 K with a time step of 1 fs was adopted. Snapshots at 4 ns for all RTILs are shown in Figure 1.

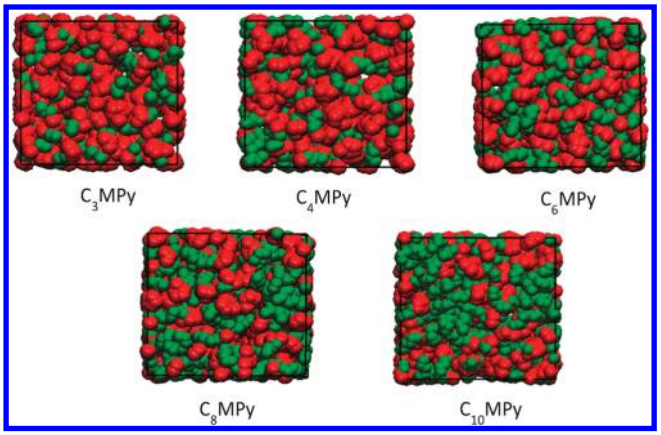

Figure 1. Snapshots of a series of ionic liquids $[C_nMPy][Tf_2N]$. Red atoms indicate the charged pyrrolidinium ring. The alkyl chains are shown as green.

It is clear that the tail groups aggregate and form several spatially heterogeneous domains. The domains grow larger with increasing alkyl chain length of the cationic $[C_nMPy]^+$. The intermolecular center of mass (COM) site−site radial distribution functions (RDFs) were calculated as shown in Figure S1 of the Supporting Information. Initially, we assumed the cations would assemble through tail aggregation in $[C_nMPy][Tf_2N]$ as the alkyl chain length was increased, similar to the phenomenon reported in imidazolium-based ionic liquids. Surprisingly, the calculated cation−cation RDF decreases with increasing n, while the peak shifts to longer distances (Figure S1a). These results suggest that a longer alkyl chain does not cause cation aggregation. On the contrary, the cations are more spatially separated as n was increased. This is possibly due to the shift of cation COM. With increasing alkyl chain length, the COM is shifted toward the alkyl chains. Nevertheless, the length of the side alkyl chain of the cation does not affect the anion−anion radial distribution (Figure S1b). The cation−anion RDF is greatly decreased with increasing n (Figure S1c). To exclude the effects of the alkyl chain on the COM of the cation, we calculated the RDF of the pyrrolidinium ring relative to the COM of the anion. An opposite trend, in which the correlation of ring−anion increases with increased alkyl chain length, was observed (Figure S1d). This phenomenon agrees with Margulis' report on imidazolium-based ionic liquids.[9] The RDF of the alkyl side-chain terminal carbon is typically the most direct evidence of alkyl tail aggregation. However, no evident differentiation among $[C_6MPy]^+$, $[C_8MPy]^+$, and $[C_{10}MPy]^+$ was observed (Figure S2), in contrast to reports on imidazolium-based ILs.[7,9] Although the RDF of the terminal carbon does not clearly show the expected behavior, the coordination number increases as n increases, from 3 for n = 3 to 6.8 for n = 10, which indicates the enhancement of aggregation behavior.

To further explore the effects of alkyl chain length on the liquid structure of $[C_nMPy][Tf_2N]$, the structure function $S(Q)$ of all five ILs was calculated and compared with SAXS results, as shown in Figure 2a. For scattering at low values of wave

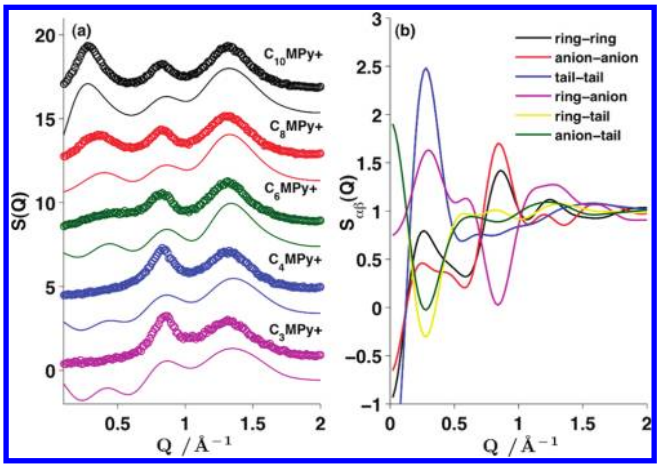

Figure 2. (a) Structure functions for n = 3, 4, 6, 8, 10 $[C_nMPy][Tf_2N]$ measured at room temperature. Open symbols in varying colors represent SAXS results; the solid lines with corresponding colors represent MD calculated results. (b) Partial structure functions contributed by varying site−site correlations of $[C_{10}MPy][Tf_2N]$ calculated from MD simulation at 298 K. Here the ring is defined as the center of mass of the pyrrolidinium ring; the tail is defined as the terminal carbon of alkyl chain.

vector transfer in ionic liquids, sources of higher electron density are needed in order to provide good X-ray contrast. The cation ring and the corresponding anion in $[C_nMPy][Tf_2N]$ are closely bound, forming a polar group in the ionic liquid that provides excellent X-ray contrast with neighboring alkyl chains. Our SAXS provided information with a 0.01−2.8 $Å^{-1}$ Q range, covering both intermolecular and large-scale intramolecular length scales.

Three peaks were observed as shown in Figure 2a; for example, for n = 10, peaks occur near 1.35, 0.8, and 0.3 $Å^{-1}$. Figure 2b is the unweighted partial structure functions for n = 10 calculated by Fourier transformation of corresponding MD-generated site−site RDFs of $[C_nMPy][Tf_2N]$. We first consider the peak near 1.35 $Å^{-1}$, corresponding to the real space distance of $2\pi/1.35$ = 4.65 Å, which is close to the ring−anion correlation. Figure 2b explicitly shows that the strongest contribution to the peak near 1.35 $Å^{-1}$ is from the ring−anion correlations, which is consistent with Aoun's computational result on $[C_nmim+]$[17,23] and Santos' X-ray scattering study on $[C_nMPy][Tf_2N]$.[20] We now consider the two peaks near 0.8 and 0.3 $Å^{-1}$. Peaks that arise at low Q values, or FSDPs, are a prominent feature in network glasses and typically interpreted as a sign of intermediate range order.[24−28] Two main trends are

dx.doi.org/10.1021/jz2013209 | J. Phys. Chem.Lett. 2012, 3, 125−130

immediately evident from observation of $S(Q)$ within $Q < 1$ Å^{-1}. First, a strong alkyl chain-dependent FSDP (see Figure 2b) occurs (clearly defined at ~0.29 Å^{-} for $n = 10$). This FSDP drops in intensity and shifts toward higher Q (0.36 Å^{-1} for $n = 8$ and 0.47 Å^{-1} for $n = 6$) and decreases in intensity as the alkyl chain length is shortened so that its contribution at $n = 4$ and $n = 3$ is weak as shown in Figure 3b. Second, Figure 2b shows

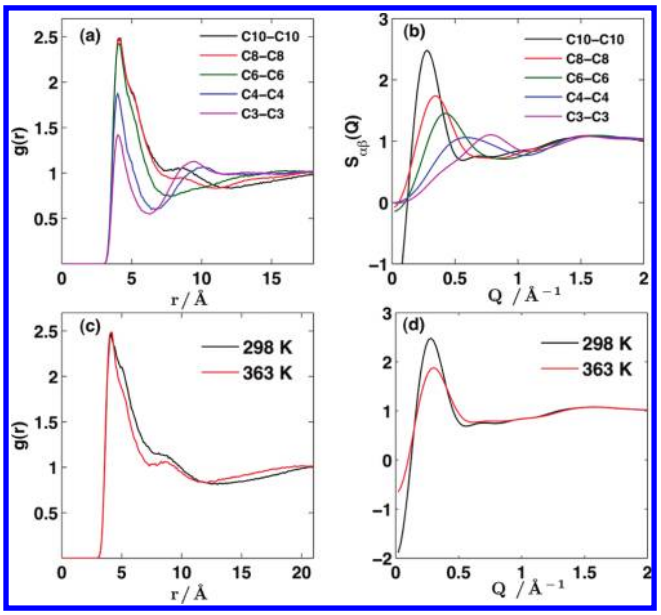

Figure 3. (a) Tail−tail correlation functions of $[C_nMPy][Tf_2N]$. (b) The corresponding partial structure functions of (a). (c) Tail−tail correlation functions of $[C_{10}MPy][Tf_2N]$ as a function of temperature. (d) The corresponding partial structure functions of (c) calculated at 298 and 363 K.

that at 0.8 Å^{-1}, corresponding to a real space distance of 7.8 Å, positive contributions from the cation ring−ring and anion−anion correlation along with a negative contribution from the cation ring−anion correlation are present. This is similar to what has been observed in imidazolium-based ionic liquids[29,30] with Cl and PF_6 anions and is a clear sign of the charge ordering in this system. Figure S1 shows the deep valley in the cation−anion real space correlation function (Figure S1c) that corresponds to the distance between the like-charged species (Figure S1a). Since the peak near 0.8 Å^{-1} in Figure 2a does not change in position substantially as the alkyl chain length is decreased, it appears that the low-Q peak near 0.3 Å^{-1} merges with the second polar group peak near 0.8 Å^{-1} noted by the slight yet systematic increase of the second peak's intensity as the chain length is decreased. These low-Q features can provide insight into the large-scale organization of the $[C_nMPy][Tf_2N]$ system.

The X-ray-weighted subcomponents of partial structure function contributed by cation−cation, cation−anion, and anion−anion correlations (Figure S3a) were calculated using Santos's method.[15] As reported by Annapureddy et al.[29] for imidazolium-based RTILs, our results suggest that anion−anion correlations contribute positively to the positive FSDP and the second peak located at 0.8 Å^{-1}. Negative contribution to the peaks results from the cation−anion correlation. The atomic partial structure factor was then calculated as shown in Figure S3b, which demonstrated that the positive FSDP was mainly from cross-atom correlations in anions. However, carbon−carbon and hydrogen−hydrogen correlations barely contribute to the structure function. These findings are in agreement with our above analysis.

The results of several experimental and computational investigations have been recently combined by Annapureddy et al.[29,30] Their study identifies the origin of the prepeak in imidazolium-based ionic liquids and offers a way to describe liquid-state structural observations based on observed crystallographic ordering. Although the crystalline and liquid states are not the same, this approach nevertheless helps to understand the scattering measurements. A similar approach is used here to describe the alkyl chain-dependent experimental observations in our pyrrolidinium system. We define I_E as the structural peak corresponding to the nearest-neighbor polar group separation, which is primarily governed by electrostatic interactions, and I_A as corresponding to the alkyl chain-separated polar group distance.

Analysis of the peak positions and intensities in the SAXS data for $Q < 1$ Å^{-1} for the series in this study yields some interesting trends. These were obtained by fitting two Gaussian functions with a quadratic baseline, in a manner similar to other studies,[28,29] which fit the data well. More information is provided in Figure S4 of the Supporting Information along with the results of these fits provided as plots of the peak position, as well as peak height, as a function of alkyl chain length. The peak positions for samples with $n = 6$ to $n = 10$ lie on a line with a slope of 2 Å per CH_2 group. The low-Q peak I_A centers for $n = 3$ to $n = 10$ (Figure S4a) convert to real space values between 8.8 and 22 Å, respectively, corresponding to the peaks lying on a line of slope (22 Å − 8.8 Å)/7 = 1.9 Å per CH_2 group; focusing just on samples with $n = 6$ to $n = 10$, the slope is 2 Å per CH_2 group. Hence, the measured alkyl chain-separated polar group distance for a given n is less than twice that of an all-trans n-alkyl chain for all the ionic liquids. This suggests some level of interdigitization[29,30] or coiling of the alkyl chains, especially for the longer alkyl chain liquids. The low-Q I_A peak contribution (see Figure S4b) is clearly visible for $n = 10$ and 8 but less obvious for $n = 6$, 4, and 3. From the low-Q I_A peak analysis (see Figure S4a) we obtain peak positions corresponding to distances of 13.3, 9.6, and 8.8 Å for $n = 6$, 4, and 3, respectively, for the alkyl-chain-separated polar group distance. As the alkyl chain length decreases, it is clear that this dimension approaches the near-neighbor polar group separation distance of 7.8 Å (i.e., I_E peak) which shows no significant alkyl chain length dependence. Thus, the I_E peak at 0.8 Å^{-1} shows a systematic increase in intensity with decreasing alkyl chain length, while the low-Q I_A peak is diminished (Figure 2 and Figure S4). These observations are consistent with previous reports on the alkyl chain length dependence of the low-Q scattering in imidazolium-based RTILs.[17,29]

Figure 3b shows that the tail−tail correlations contribute to the FSDP, especially for longer chain $[C_nMPy][Tf_2N]$. The main peak in the tail−tail partial structure functions coincides with the peaks of other partials involving the anions, cations, and tails, and while other correlations play a dominant role due to their electronic weights as shown in Figure S3, it is nevertheless present and plays a role in the organization of the charged species in the system. The contribution of tail−tail correlations to I_A is smaller for $n < 6$, and the peak position shifts to higher Q with a decrease in n. These results show that longer alkyl chains greatly favor tail−tail assembly as reported in the FCS experiments.[21] For chain length $n < 6$, the alkyl

dx.doi.org/10.1021/jz2013209 | J. Phys. Chem.Lett. 2012, 3, 125−130

chain van der Waals forces cannot overcome the electrostatic forces to exhibit closer association.

The temperature effects on the structure functions of $[C_nMPy][Tf_2N]$ obtained from both simulation and SAXS are shown in Figure 4. It is common to observe broadening of

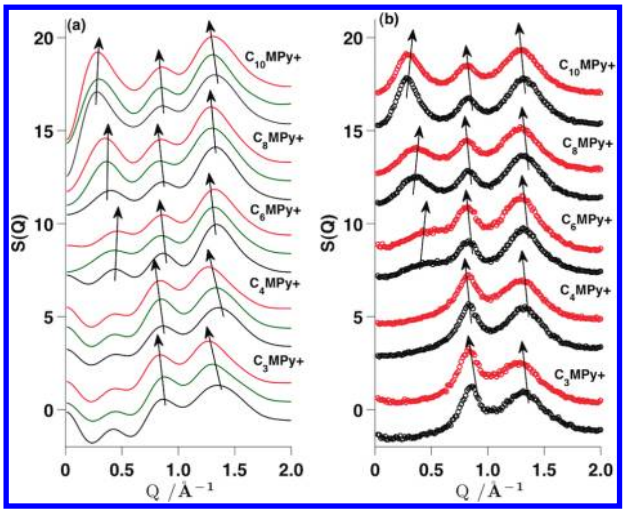

Figure 4. MD (a) and SAXS (b) curves showing the temperature dependence of structure factors for $[C_nMPy][Tf_2N]$. Black symbols denote MD/SAXS results at 298 K, green symbols denote MD/SAXS results at 348 K, and red symbols denote MD/SAXS results at 363 K. The curves have been offset vertically for clarity. The second and third peaks shift toward lower Q values as the temperature is increased; however, the alkyl-chain-separated polar group peak shifts toward higher Q with increasing temperature for n = 6, 8, and 10.

diffraction peaks as the temperature is raised in a liquid.[31−33] The shift of diffraction peaks to lower Q values is a feature that correlates with a density decrease[20] as intra- and intermolecular distances increase. These observations hold for the current series under investigation, with the exception of the alkyl chain-dependent peak, I_A. For n = 8 and 10, there is a clear shift of this FSDP to higher Q with increasing temperature (Figure 4). For n = 3, 4, and 6, this effect, if present, is very slight.

The work reported by Triolo on $[C_nmim][BF_4]$ with n = 3−10 exhibits a similar trend in the supercooled liquid in the range from 90 to 290 K.[13] For temperatures above the glass transition, T_g, they attribute a spatial correlation decrease with increasing temperature to diffusion, and when diffusive processes are arrested below T_g, then the peak shift is strictly related to density changes. In order to reveal the temperature effects on the FSDP position, the temperature-dependent tail−tail correlation was analyzed. Figure 3c displays calculated tail−tail correlations for $[C_{10}MPy][Tf_2N]$ at varying temperatures and the corresponding $S(Q)$s in Figure 3d. As the temperature was raised, the FSDP shifted to higher Q; no significant change in the first- and second-neighbor position occurs, but an increase in the ordering between the tails does occur as indicated by the narrowing in the correlation peak. Also, the tail−tail coordination number calculated by integration of its correlation from 0 to 12 Å decreased from 11.6 at 298 K to 10.8 at 363 K, which may be crucial for an understanding of the temperature-dependent FSDP shift. The changes in the peak position from 298 to 363 K as a function of chain length, n, are plotted in the Supporting Information (Figure S5). The negative values correspond to shifts toward lower Q and positive values toward higher Q as the temperature was increased. For n = 10, the shift over this temperature range was 0.013 Å^{-1}.

The following is an interpretation of our observations. Because of the increased interaction between alkyl chains as the chain length is increased (shown in the present simulation, Figure 3), the alkyl chains play a significant role in the ordering of the liquid. There is, in effect, competition between the strong charge ordering of the ions and the weaker van der Waals influence of the alkyl chains. At ambient temperatures, the van der Waals interactions are stronger for the long alkyl chain liquids and increase chain association. However, at higher temperatures, the van der Waals interactions are reduced and the polar group electrostatic forces dominate. At higher temperatures it is more likely for a cation tail to diffuse[13] from its nonpolar aggregate, thus resulting in a decrease in the aggregate size shown by the slight shortening of the alkyl-chain-separated polar group distance (Figure 4). The diffusion step is necessary to preserve first-neighbor ionic distances, since they are dependent on the density rather than the temperature. This reduction in aggregate size will result in shorter chain aggregate correlation distances, indicated by the shift to higher Q values in the tail−tail partial $S(Q)$ (Figure 3b).

MD simulations, as shown in the snapshot at 4 ns (Figure 1) and the RDFs (Figure 3b), clearly demonstrate that the aggregation size increases with increasing alkyl chain length, consistent with our FCS findings.[21] The FCS results showed evidence for self-aggregation domains for $[C_3mpy][Tf_2N]$, and SAXS experiments show evidence of the existence of an alkyl chain-dependent weak polar group ordering, I_A, for n = 3 and 4. MD simulations suggest the averaged aggregation size for $[C_3MPy][Tf_2N]$ is ∼3 alkyl chains. All the techniques unambiguously show the self-aggregation for n > 4.

Structural heterogeneity in ILs has been a subject of considerable attention in the past few years. It has been reported that long chain $[C_nmim+]$ (n > 12) systems or alcohols can form micelle-like structures easily. The self-aggregation of midrange alkyl chain $[C_nmim+]$ systems was first suggested by MD simulations from Voth et al.[7] and supported by SAXS from Triolio et al.[13,14] Hardacre and co-workers[17] called the meaning of the FSDP peak into question through well-designed SANS experiments based on selectively H/D-isotopically substituted $[C_nmim+]$ systems. Other experimental evidence, such as the observation of pronounced "hyper-polarity", biphasic diffusion dynamics observed using FCS, and rotational dynamics probed by optical heterodyne-detected Raman-induced Kerr effect spectroscopy,[12] point to self-aggregation, or locally ordered domains/structures, or micro-phase separation of ionic liquids. The results from our MD simulation support the aggregation of alkyl chains in $[C_nMPy][Tf_2N]$, as evidenced by the snapshot in Figure 1. The SAXS measurements in turn highlight the ordering of the polar groups that results from both electrostatic ion ordering at short distance and the complex alkyl chain interactions at further distances. More carefully designed SANS experiments with different H/D-isotropically exchanged $[C_nMPy][Tf_2N]$ as well as rotation dynamics of dyes in $[C_nMPy][Tf_2N]$ probed by fluorescence anisotropy spectroscopy will be reported elsewhere.

In summary, molecular modeling and small-angle X-ray scattering were applied to elucidate the alkyl chain length and temperature effects on the nanoscale organization of pyrrolidinium-based ionic liquids. For the first time, we demonstrated that the cation tails of pyrrolidinium-based

dx.doi.org/10.1021/jz2013209 | J. Phys. Chem.Lett. 2012, 3, 125−130

ionic liquids with long alkyl chains exhibit aggregation behavior which is analogous to imidazolium-based ionic liquids. The alkyl chain segregation is attributed to electrostatic interactions between polar groups and van der Waals forces of the nonpolar alkyl chains.

■ ASSOCIATED CONTENT

Supporting Information

Methodology details and supplementary figures. This material is available free of charge via the Internet at http://pubs.acs.org.

■ AUTHOR INFORMATION

Corresponding Author

*E-mail peter.cummings@vanderbilt.edu, Tel 615-322-8129, Fax 615-343-7951.

■ ACKNOWLEDGMENTS

This work was supported as part of the Fluid Interface Reactions, Structures, and Transport (FIRST) Center, an Energy Frontier Research Center funded by the U.S. Department of Energy, Office of Science, Office of Basic Energy Sciences. A portion of this research was conducted at the Center for Nanophase Materials Sciences, which is sponsored at Oak Ridge National Laboratory by the Office of Basic Energy Sciences, U.S. Department of Energy. One of the authors, S.L., gratefully acknowledges Oleg Borodin and Grant Smith for graciously providing the APPLE&P force field parameters used in this work. We also would like to pay great appreciation to Adam J. Rondinone and Andrew Payzant for their kind assistance in SAXS measurement.

■ REFERENCES

(1) Tsuda, T.; Hussey, C. L. Electrochemical Applications of Room-Temperature Ionic Liquids. *Electrochem. Soc. Interface* **2007**, *16*, 42−49.

(2) Earle, M. J.; Seddon, K. R. Ionic Liquids. Green Solvents for the Future. *Pure Appl. Chem.* **2000**, *72*, 1391−1398.

(3) Davis, J. H. Task-Specific Ionic Liquids. *Chem. Lett.* **2004**, *33*, 1072−1077.

(4) Xiao, D.; Hines, L. G.; Li, S. F.; Bartsch, R. A.; Quitevis, E. L.; Russina, O.; Triolo, A. Effect of Cation Symmetry and Alkyl Chain Length on the Structure and Intermolecular Dynamics of 1,3-Dialkylimidazolium Bis(Trifluoromethanesulfonyl)Amide Ionic Liquids. *J. Phys. Chem. B* **2009**, *113*, 6426−6433.

(5) Seddon, K. R.; Stark, A.; Torres, M. J. Viscosity and Density of 1-Alkyl-3-Methylimidazolium Ionic Liquids. *Clean Solvents* **2002**, *819*, 34−49.

(6) Tokuda, H.; Hayamizu, K.; Ishii, K.; Susan, M. A.; Watanabe, M. Physicochemical Properties and Structures of Room Temperature Ionic Liquids. 2. Variation of Alkyl Chain Length in Imidazolium Cation. *J. Phys. Chem. B* **2005**, *109*, 6103−6110.

(7) Wang, Y.; Voth, G. A. Unique Spatial Heterogeneity in Ionic Liquids. *J. Am. Chem. Soc.* **2005**, *127*, 12192−12193.

(8) Wang, Y.; Voth, G. A. Tail Aggregation and Domain Diffusion in Ionic Liquids. *J. Phys. Chem. B* **2006**, *110*, 18601−18608.

(9) Margulis, C. J. Computational Study of Imidazolium-Based Ionic Solvents with Alkyl Substituents of Different Lengths. *Mol. Phys.* **2004**, *102*, 829−838.

(10) Lopes, J. N. A. C.; Padua, A. A. H. Nanostructural Organization in Ionic Liquids. *J. Phys. Chem. B* **2006**, *110*, 3330−3335.

(11) Bradley, A. E.; Hardacre, C.; Holbrey, J. D.; Johnston, S.; McMath, S. E. J.; Nieuwenhuyzen, M. Small-Angle X-Ray Scattering Studies of Liquid Crystalline 1-Alkyl-3-methylimidazolium Salts. *Chem. Mater.* **2002**, *14*, 629−635.

(12) Russina, O.; Triolo, A.; Gontrani, L.; Caminiti, R.; Xiao, D.; L., G. H. Jr.; Bartsch, R. A.; Quitevis, E. L.; Plechkova, N.; Seddon, K. R. Morphology and Intermolecular Dynamics of 1-Alkyl-3-methylimidazolium Bis{(trifluoromethane)sulfonyl}amide Ionic Liquids: Structural and Dynamic Evidence of Nanoscale Segregation. *J. Phys.: Condens. Matter* **2009**, *21*, 424121.

(13) Triolo, A.; Russina, O.; Bleif, H. J.; Di Cola, E. Nanoscale Segregation in Room Temperature Ionic Liquids. *J. Phys. Chem. B* **2007**, *111*, 4641−4644.

(14) Triolo, A.; Russina, O.; Fazio, B.; Triolo, R.; Di Cola, E. Morphology of 1-Alkyl-3-methylimidazolium Hexafluorophosphate Room Temperature Ionic Liquids. *Chem. Phys. Lett.* **2008**, *457*, 362−365.

(15) Santos, C. S.; Annapureddy, H. V. R.; Murthy, N. S.; Kashyap, H. K.; Castner, E. W.; Margulis, C. J. Temperature-Dependent Structure of Methyltributylammonium Bis(trifluoromethylsulfonyl)-amide: X Ray Scattering and Simulations. *J. Chem. Phys.* **2011**, *134*, 064501.

(16) Zheng, W.; Mohammed, A.; Hines, L. G.; Xiao, D.; Martinez, O. J.; Bartsch, R. A.; Simon, S. L.; Russina, O.; Triolo, A.; Quitevis, E. L. Effect of Cation Symmetry on the Morphology and Physicochemical Properties of Imidazolium Ionic Liquids. *J. Phys. Chem. B* **2011**, *115*, 6572−6584.

(17) Hardacre, C.; Holbrey, J. D.; Mullan, C. L.; Youngs, T. G.; Bowron, D. T. Small Angle Neutron Scattering from 1-Alkyl-3-methylimidazolium Hexafluorophosphate Ionic Liquids ([C(N)Mim]-[Pf(6)], N = 4, 6, and 8). *J. Chem. Phys.* **2010**, *133*, 074510.

(18) Macchiagodena, M.; Gontrani, L.; Ramondo, F.; Triolo, A.; Caminiti, R. Liquid Structure of 1-Alkyl-3-methylimidazolium-Hexafluorophosphates by Wide Angle X-Ray and Neutron Scattering and Molecular Dynamics. *J. Chem. Phys.* **2011**, *134*, 114521.

(19) Taige, T.; Schubert, T. J. S. Physico-Chemical Properties of Ionic Liquids-Part I. *Ionic Liq. Today* **2011**, *1−11*, 4−10.

(20) Santos, C. S.; Murthy, N. S.; Baker, G. A.; Castner, E. W. Communication: X-Ray Scattering from Ionic Liquids with Pyrrolidinium Cations. *J. Chem. Phys.* **2011**, *134*, 121101−121104.

(21) Guo, J.; Baker, G. A.; Hillesheim, P. C.; Dai, S.; Shaw, R. W.; Mahurin, S. M. Fluorescence Correlation Spectroscopy Evidence for Structural Heterogeneity in Ionic Liquids. *Phys. Chem. Chem. Phys.* **2011**, *13*, 12395−12398.

(22) Borodin, O. Polarizable Force Field Development and Molecular Dynamics Simulations of Ionic Liquids. *J. Phys. Chem. B* **2009**, *113*, 11463−11478.

(23) Saboungi, M. L.; Aoun, B.; Goldbach, A.; Gonzalez, M. A.; Kohara, S.; Price, D. L. Nanoscale Heterogeneity in Alkylmethylimidazolium Bromide Ionic Liquids. *J. Chem. Phys.* **2011**, *134*, 104509.

(24) Wilson, M.; Madden, P. A. Prepeaks and 1st Sharp Diffraction Peaks in Computer-Simulations of Strong and Fragile Ionic Liquids. *Phys. Rev. Lett.* **1994**, *72*, 3033−3036.

(25) Urahata, S. M.; Ribeiro, M. C. Structure of Ionic Liquids of 1-Alkyl-3-methylimidazolium Cations: A Systematic Computer Simulation Study. *J. Chem. Phys.* **2004**, *120*, 1855−1863.

(26) Tosi, M. P.; Price, D. L.; Saboungi, M. L. Ordering in Metal Halide Melts. *Annu. Rev. Phys. Chem.* **1993**, *44*, 173−211.

(27) Mei, Q.; Benmore, C. J.; Weber, J. K. Structure of Liquid SiO2: A Measurement by High-Energy X-Ray Diffraction. *Phys. Rev. Lett.* **2007**, *98*, 057802.

(28) Bychkov, E.; Benmore, C. J.; Price, D. L. Compositional Changes of the First Sharp Diffraction Peak in Binary Selenide Glasses. *Phys. Rev. B* **2005**, *72*, 172107.

(29) Annapureddy, H. V. R.; Kashyap, H. K.; De Biase, P. M.; Margulis, C. J. What Is the Origin of the Prepeak in the X-Ray Scattering of Imidazolium-Based Room-Temperature Ionic Liquids? *J. Phys. Chem. B* **2010**, *114*, 16383−16846.

(30) Annapureddy, H. V. R.; Kashyap, H. K.; De Biase, P. M.; Margulis, C. J. What Is the Origin of the Prepeak in the X-Ray Scattering of Imidazolium-Based Room-Temperature Ionic Liquids? *J. Phys. Chem. B* **2011**, *115*, 9507−9508.

(31) Lin, C.; Busse, L. E.; Nagel, S. R.; Faber, J. Temperature Dependence of the Structure Factor of Ges2 Glass. *Phys. Rev. B* **1984**, *29*, 5060−5062.
(32) Busse, L. E.; Nagel, S. R. Temperature Dependence of the Structure Factor of As2se3 Glass up to the Glass Transition. *Phys. Rev. Lett.* **1981**, *47*, 1848−1851.
(33) Susman, S.; Volin, K. J.; Montague, D. G.; Price, D. L. The Structure of Vitreous and Liquid Gese2: A Neutron Diffraction Study. *J. Non-Cryst. Solids* **1990**, *125*, 168−180.